Exploring the Novice Approach to Orthorectification of Satellite Imagery

G. Mallikarjuna Rao, Ch. Mallikarjuna Rao, B. R. K. Reddy, D. V. Lalitha Parameswari and Mohammad Azeez

Abstract Orthorectification plays vital role in satellite image processing. This process imposes challenges due to the dynamism in capturing environment, capturing unit, satellite rotation, sensors parameters and overlying regions on earth. The required geometric modelling needs an accurate estimation of Ground Control Points (GCPs) and their processing. Most of the proposed models are computational intensive and use manual approach for locating GCPs. Further, GCPs co-ordinates are floating point numbers the computational capability of the system imposes the constraint on the accuracy and robustness of the respective models. In this paper we have studied orthorectification process and proposed instinctive processing framework for orthorectification of optical pushbroom sensor based satellite imagery. The frame work accompany metadata extraction, automatic ground control point (GCP) extraction using parallel processing, geometric modeling, orthorectification and image stitching processes. Experimental results with proposed framework confirmed the robustness of the technique and provided sub pixel accuracy on independent check points with positional accuracy around one pixel for orthoimage. Parallel SIFT features are extracted using SIMD architecture while performing image stitching.

Keywords Orthorectification · Generic geometric model · Ground control point (GCP) · Optical imagery · Random sample (RANSAC)

G. Mallikarjuna Rao (✉) · Ch. Mallikarjuna Rao · B. R. K. Reddy · M. Azeez
Gokaraju Rangaraju Institute of Engineering and Technology, Hyderabad, India
e-mail: Gmr_333@yahoo.com

Ch. Mallikarjuna Rao
e-mail: chmksharma@yahoo.com

D. V. Lalitha Parameswari
G. Narayanamma Institute of Technology and Science, Hyderabad, India

1 Introduction

The base map layer, a visual source, provided by satellite images is used as statistical analysis tool for disaster predictions and management, change detection and digital analysis. However some applications such as disaster prediction and man-agreement, require visual and accuracy factors of satellite image while the other applications such as military and navigation, needs location accuracy as main consideration. Radiometric (spectral) and geometric (spatial) corrections are performed to improve visual and accuracy properties. These operations require considerable computational effort and better resolution of satellite image.

1.1 Over View of the Development

The four basic components of orthorectification are (1) raw image (2) geometric model (3) DEM (digital elevation model) (4) GCP (ground control points). Orthorectification of satellite imagery imposes challenges due to the dynamism in capturing environment, capturing unit, satellite rotation, sensors parameters and overlying regions on earth. Further pixel positional displacements are common problems due to lens distortion and camera tilt. Orthorectification models [1–3, 9, 16] have taken care about positional displacement of pixels by employing real-ground co-ordinates (including x, y and z values). However these floating point co-ordinate vales have to be properly processed to provide pixel values of the orthoimage. Thus computational environment capability influences the accuracy. The geometric correction using geometric rectification and orthorectification is a common practice [6–8, 15] in the modern remote sensing (RS) to provide accurate orthoimage. Digital Elevation Model (DEM) along with GCPs (link between image and ground co-ordinate) is used for this purpose. However, the main challenge here is to capture the appropriate number of high quality GCPs and selection of correct quality of DEM. Some of the orthorectification models are:

(i) Polynomial rectification models: Polynomial function is applied to the surface adapt the polynomial to a number of check point is one the simplest image processing method to cancel the effects of tilts for both satellite images and aerial photographs. However the polynomial order is greatly influenced by number of GCPs and desired accuracy.

(ii) Rational Polynomial satellite sensor models: these models uses ratio of two cubic polynomial expressions and provide empirical mathematical models relating image coordinates (row and column position) to latitude and longitude using the terrain surface elevation. The coefficients of these two cubic polynomials (one for row and another for column) are computed by Satellite Company from satellite's orbital position, and orientation. Automatic Resampling Geometric relationship between object space and image space is provided by rational function sensor model. It relates object point coordinates (X,

Y, *Z*) to image pixel coordinates row and column (*r*, *c*) or vice versa using 78 rational polynomial coefficients (RPCs). Following Eqs. 1 and 2 provide the ground-to-image transformation:

$$r_n = \frac{p_1(X_n, Y_n, Z_n)}{p_2(X_n, Y_n, Z_n)} = \frac{\sum_{i=0}^{m1} \sum_{j=0}^{m2} \sum_{k=0}^{m3} a_{ijk} X_n^i Y_n^j Z_n^k}{\sum_{i=0}^{m1} \sum_{j=0}^{m2} \sum_{k=0}^{m3} b_{ijk} X_n^i Y_n^j Z_n^k} \tag{1}$$

$$c_n = \frac{p_1(X_n, Y_n, Z_n)}{p_2(X_n, Y_n, Z_n)} = \frac{\sum_{i=0}^{m1} \sum_{j=0}^{m2} \sum_{k=0}^{m3} c_{ijk} X_n^i Y_n^j Z_n^k}{\sum_{i=0}^{m1} \sum_{j=0}^{m2} \sum_{k=0}^{m3} d_{ijk} X_n^i Y_n^j Z_n^k} \tag{2}$$

In the above expressions $a_{ijk}, b_{ijk}, c_{ijk},$ and d_{ijk} denote Rational Function Coefficients, while (r_n, c_n) denote image space normalized row (line) and column (sample) index of pixels. Normalized coordinate values of object points in ground space are denoted by $X_n, Y_n,$ and Z_n. However, subjective procedure of selecting control points and associated RMS error of residue vales imposes limitation on achievable accuracy.

(iii) Projective rectification: It uses a geometric transformation between the image plane and the projective plane. At least four control points in the object plane are required to compute eight unknown coefficients, b_{ij}, using projective transformation. The row and column (*r*, *c*) are computed as per following expressions

$$r = \frac{b_{11}x + b_{21}y + b_{31}}{b_{12}x + b_{23}y + 1} \tag{3}$$

$$c = \frac{b_{12}x + b_{22}y + b_{31}}{b_{13}x + b_{23}y + 1}. \tag{4}$$

In general, orthorectifying low-to medium resolution (L-MR) satellite imagery Shuttle Radar Topography Mission (SRTM) 30 m DEM is sufficient while high-resolution (HR) and very high-resolution (VHR) satellite imagery require DEM with 15 m or less GSD (ground sample distance) is needed [4, 5, 15]. In our experimentation Ground Controls Points are manually collected with GeoExplorer 6000 series handheld (model: GeoXH 3.5G) receiver device and automatic extraction of GCP on earth surface was done using TerraSAR-1 with 1 m accuracy and TerraSAR-3 with 3 m accuracy. In our modest effort it is aimed to create an optimal accurate orthoimage, having smallest root mean square error (RMSE) and positional accuracy that could be used for benchmarking as well as reference source for quantifying created orthoimage set [7, 12, 14].

Inspiration: Pixel shift due to earth curvature is addressed by orthorectification while horizontal position of image positions is addressed by georeferencing and geotectification. For each pixel orhtorecification provide *X*, *Y*, *Z* ground coordinate values. In the rectification process the ground control points and associated surface

Table 1 Different DEMs and their resolution

DEM	Resolution
Shuttle radar topography mission (SRTM)	1 arc-second (30 m)
	3 arc-second (90 m)
Digital terrain elevation data (DTED)	Level 0: 900 m; Level 1: 90 m; Level 2: 30 m
Advanced Spaceborne thermal emission and reflection radiometer (ASTER)	30 m
Global digital elevation map (GEDM)	30 m

elevation reference plays a pivotal role and responsible for providing image and ground coordinate link. The following Table 1 gives some of the public products of DEM.

The main problem here, is qualitative GCPs selection. This may due to the dearth of available resources of GCP, expensiveness associated with collection of new GCPs and inaccessibility of the specific areas in some cases it is even impossible. Some of the limitations of manually collected GCPs are:

(1) *Time overwhelming*: Covering vast area by physically visiting is not only time consuming but also difficult to reach due to environmental conditions and access restrictions.
(2) *Monetary Impact*: To embark on such a project will have a high monetary impact on logistic facilities.
(3) *Travelling constraints*: International immigration constraints have to be faced while collecting necessary information from other countries.
(4) *Terrain restrictions*: Some terrain are not conducive to provide sufficient GCPs.

2 Experimentation

In general, orthorectification demand uniform distribution with complete image covering GCPs. However, exact number of required GCPs reliant on several aspects. Some of the factors deciding the count of GCPs [5, 9–11] are accuracy of usable GCPs, wide spread of GCPs, topographical characteristics and terrain variations. More than the number of GCPs, their quality and distribution will decide the efficiency of orthorectification process. In our experimentation we used the same base with varying number of GCPs and quality of DEM.

- **Data Gathering**: It associate with

  (i)   Raw satellite Image.
  (ii) Reference data set for providing tie—points between raw image and reference image.

(iii) Digital Elevation Model data source as input reference for terrain height and slope estimation.

(iv) A geometric sensor model for correcting the various errors such as data recoding errors and systematic errors arise during the capture of satellite image.

- **Data Investigation**: Data analysis was performed by following two stages:

Stage 1: Nine experiments were performed to determine the accuracy of an ortho image by means of altering the number of GCPs and the quality of the DEMs. Three experiments each with 5, 13 and 25 GCPs with 30 m DEM, 12 m DTM and 2 m DTM respectively as shown in Fig. 1. Most precise orthoimage was identified form the experimentation and used as benchmarked one for evaluating outcomes of stage 2.

Stage 2: Scenarios to simulate the lack of GCPs that are irregularly distributed across an image scene are created using a vector road layer. Figure 2 shows created the five scenarios (West, East, North, and South and Random directions) for experimental simulation. These experiments were performed on the same image used during stage 1. A methodology is deduced from the results of stage1 and stage2. This methodology is used for improving geometric precision of orthorectification to the satellite image scene having irregularly distributed and insufficient GCPs. Accuracy, reliability and validity of the results are maintained by triangulation the data results.
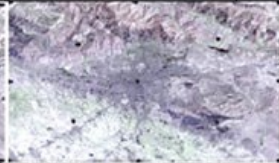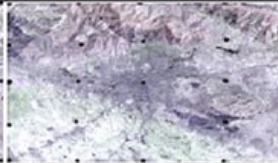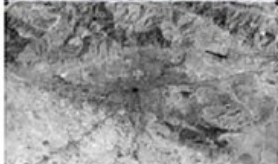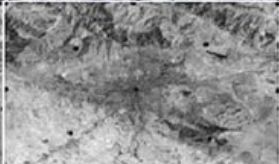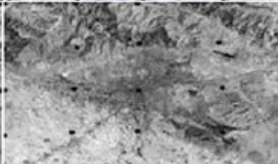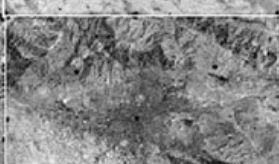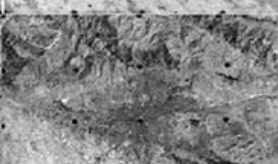

Fig. 1 Deficiency and unbalanced distribution of GCPs for several simulations
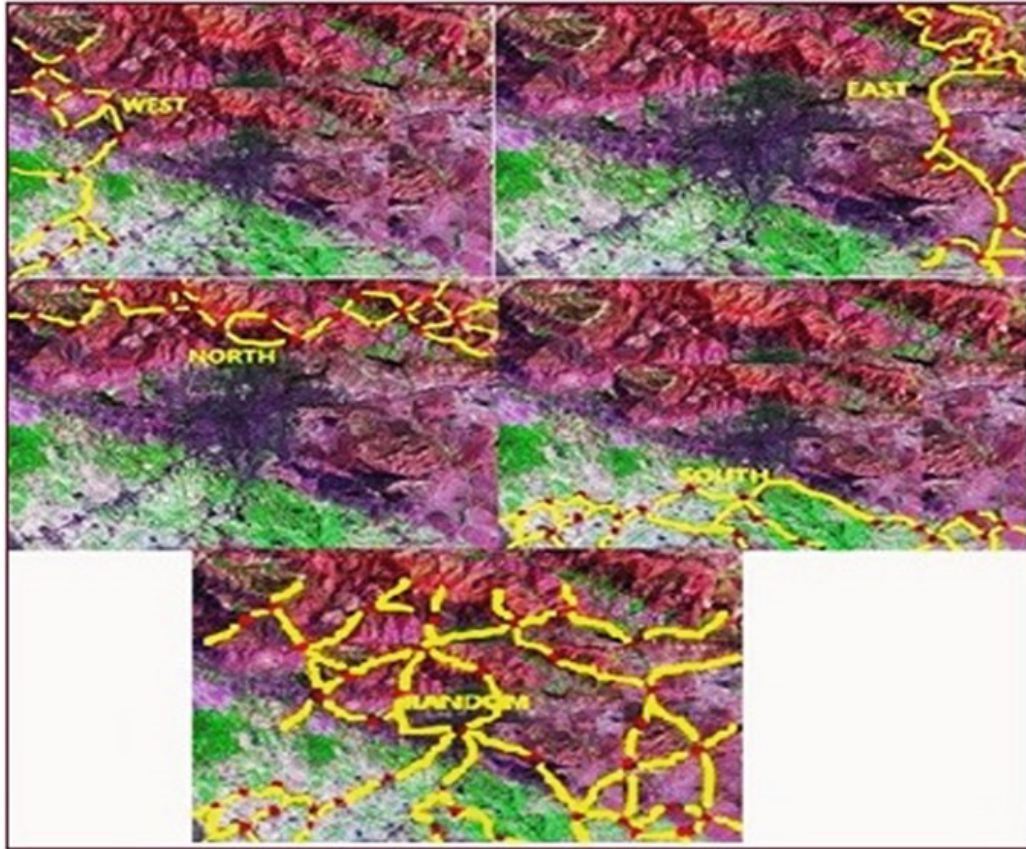
Fig. 2 DTM resolution upon varying uniformly distribute GCPs

3 Proposed Approach

The image data utilized to perform all orthorectification experiments was a Pléiades-1B primary panchromatic image. Flow diagram of the proposed frame work is given in Fig. 3.

3.1 Pseudo Code for Proposed Framework

Pseudo code used for the experimentation is given below. It is implemented ERDAS environment. Intel i7 quad core processor with 16 GB was used in the experimentation. Note that function names are given appropriately for the purpose they used and they are not directly refer any built in library function

```
1. Input: data file, f.dat in DIMP v2 structure
2. Convert_Image(f,dat)  /* this function covert the data
file into '.img' format from DIMAP XML format ERDAS
IMAGEINE@ is used*/
3. Delelte_MAP_Projected_Inf()  /*Delete the MAP and Pro-
jected information as this information is emdedded in raw
image */
4. Select_Geometric_Model() /* Pléiades Orbital Pushbroom
geometric model */
5. Add_Elevation_Model()
6. Ref_Point_Select()
/* data sources for reference point maybe GPS points,
reference images, reference files, vector files or ASCII
files */
7. Choose_out_put_format()
/* JPEG200, TIFF, IMG etc */
8. Coose_Resample_Method() /* Resampling can be done us-
ing nearest neighborhood method, bilinear interpolation,
cubic convolution or bicubic spline  */
9 Run_Orthorectification()
10 Evaluate_orthimage()
/* assess the edges of the image for sign evaluation. Ir-
regular edges denote mountain terrain*/
```

The Fig. 4 represent extraction of GCPs for various cases. However, the sensor models and elevation data were altered to match the various experiment parameters. The Fig. 5 gives final orthorectifide image with TIN DEM.

3.2 Image Stitching

If the single orthoimage of the selected resolution is not covering entire scene area then set of orthoimages are generated by above procedure are stitched to generate single orthoimage [13]. Matlab environment is used for this purpose. SIFT algorithm is used to extract key point of the images to be stitched and SIFT descriptor is used for feature or key point matching. RANSAC (Random Sample Consensus) algorithm is used to remove outliers are wrong key points and finally alpha blending is used to provide sooth mosaic image. Figure 6 indicate image stitching.

Parallel Approach for SIFT feature extraction: Let convolved image $g(x, y)$, original image is $f(x, y)$ and w is 3×3 kernel convolved image is computed as per Eq. 5.
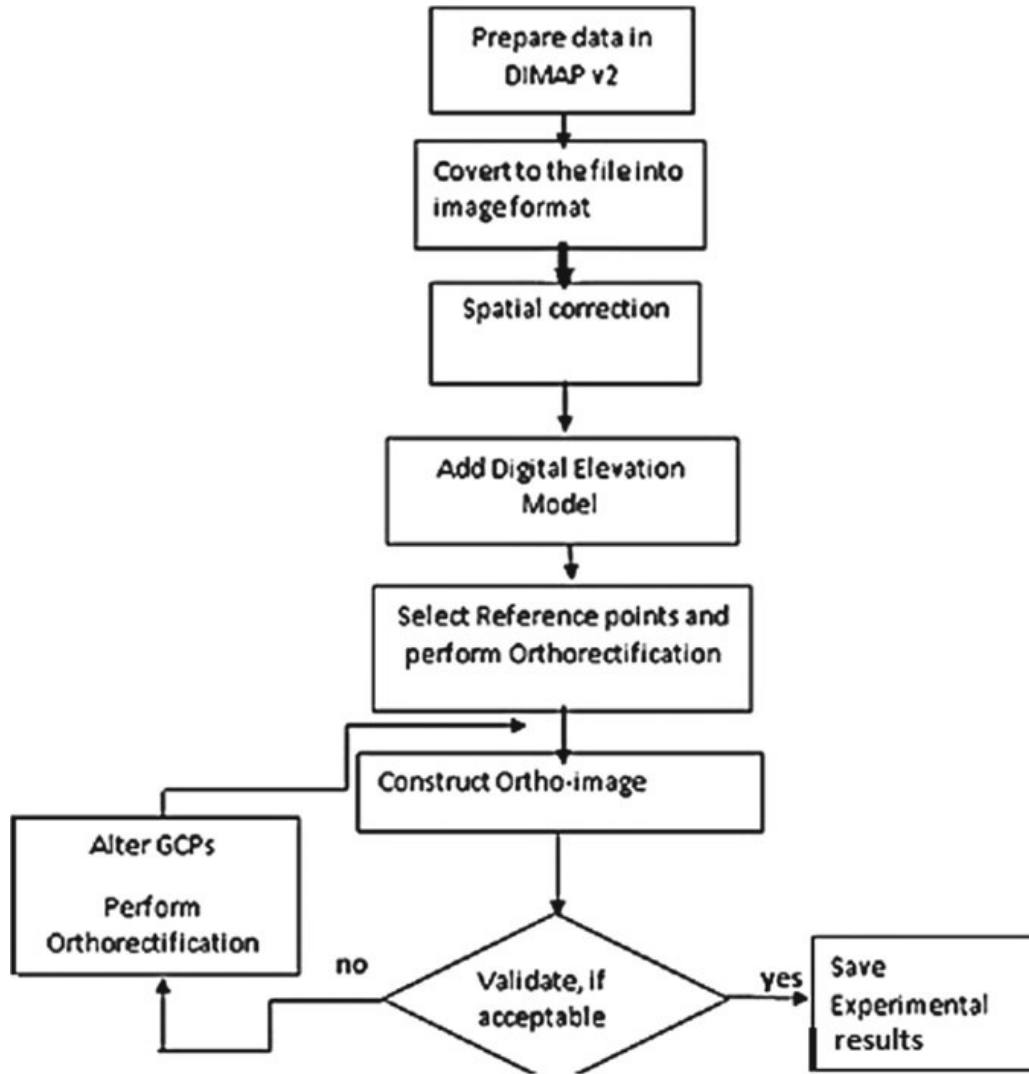
Fig. 3 Flow diagram of proposed framework

$$g(x, y) = w * f(x, y) = \sum_{s=-1}^{+1} \sum_{t=-1}^{+1} w(s, t) * f(x - s, y - t) \tag{5}$$

In our approach, each mage [1024, 756] to be processed is divided into 189, 64 × 64 sub images and one thread is proposed to each for computing associated Gaussian convolved sub image. Later all are merged to provide Single Gaussian Image. We have used quad core machine with **48** worker threads for each core. *SIMD* (Single Instruction Multiple Data) architecture was used for this purpose. Pseudo code for processing each sub image is given below.
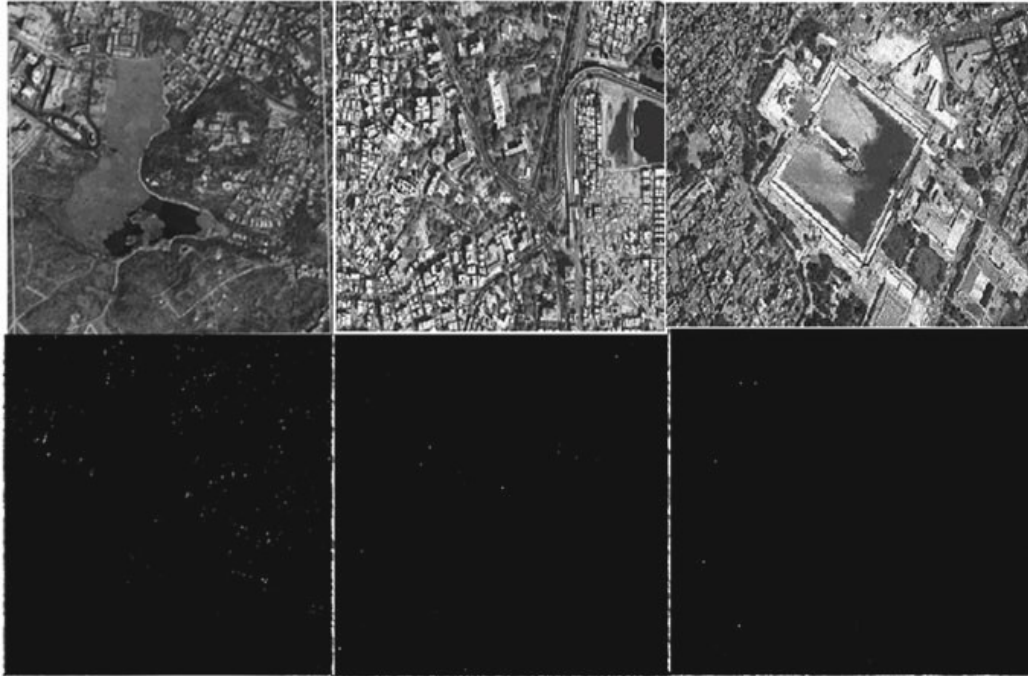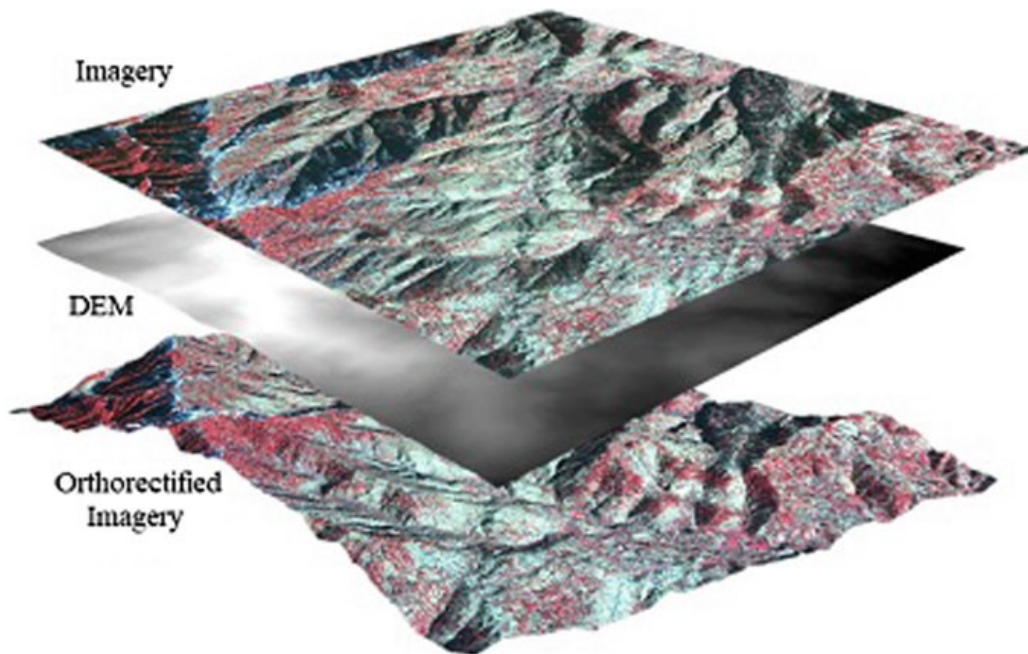
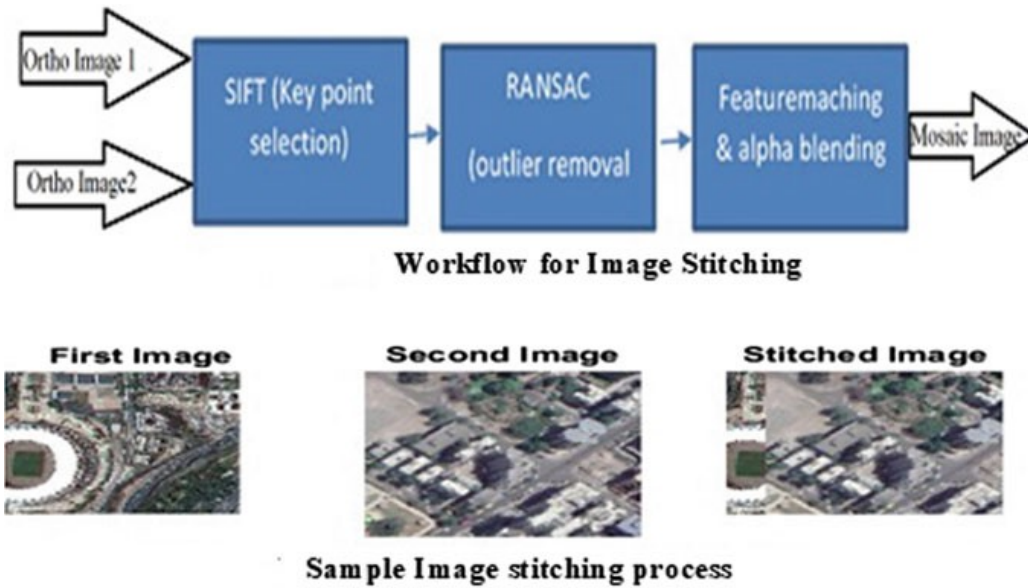**Fig. 4** GCPs for satellite images

Fig. 5 Orthorectifide image using TIN DEM

Fig. 6 Image stitching workflow

Pseudo code for Parallel Image stitching

   for each Sub_ Image S_i
    for each pixel(x,y) of S_i

    Set accum_value =0;

        for each row element of kernel

            for each column element of kernel

accum_value = accum_value + kernel(row,column)   *S_i(x-row,y-coloumn)

       end for

     endfor

    set G_i(x,y)= accum_value   /* Gaussian valve sub image region location x,y */

endfor

endfor

4 Conclusions

The presence of variables such as sensor orbital data and elevation data make it difficult to achieve absolute accuracy by mere selecting input and reference GCPs while performing orthorectification. Further accuracy is restricted by operator involvement in this process who needs to manually select and place input points (GCPs) to corresponding reference points on the primary image data. HR and VHR satellite image processing tedious task even if the precise location of the reference points is known apriori. The operator needs to identify the pixel location by zooming into pixel scale of the primary image and associate the location to the input point that correspond to the specific reference point. In this paper we analyzed the influence of number of GCPs on the acceptable orthoimage. The GCP and pixel conversion are performed in parallel using SIMD architecture. Image stitching is performed for reconstructing large orthoimage covering vast area.

References

1. Auster HU, Richter I, Glassmeier KH, Berghofer G, Carr CM, Motschmann U (2010) Magnetic field investigations during ROSETTA's 2867 Šteins flyby. Planet Space Sci 58(9):1124–1128. https://doi.org/10.1016/j.pss.2010.01.006
2. Atif S, Salman N, Irfan AI, Zahir A (2015) Accuracy assessment of digital elevation model generated from pleiades tri stereo-pair. In: 7th International conference on recent advances in space technologies, pp 193–197
3. Bhardwaj A, Sam L, Martín-Torres FJ, Kumar R, et al (2016) Uavs as remote sensing platform in glaciology: Present applications and future prospects. Remote Sens Environ, 175–196
4. Parhami B (2009) Computer arithmetic: algorithms and hardware designs, 2nd edn. Oxford University Press, Inc, New York, NY, USA
5. Becker K, Detsis E, Nwosa CC, Palevska V, Rathnasabapathy M, Taheran M (2012). Space situation awareness. In: SSS Educational series 2012.Space generation advisory council
6. Chmiel J, Kay S, Spruyt P (2004) Orthorectification and geometric quality assessment of very high spatial resolution satellite imagery for common agricultural policy purposes. In: Proceedings of XXth ISPRS congress, pp 12–23
7. Costlow T (2014) The future of satellites: what are the options? Defense systems: knowledge technology and net-enabled warfare. http://defensesystems.com/articles/2014/03/21/satellite-communications-futureptions.aspx
8. De Caro D, Genovese M, Napoli E, Petra N, Strollo AG (2014) Accurate fixed-point logarithmic converter. EEE Trans Circuits Syst II: Express Briefs 61(7):526–530
9. Ranisavljević E, Devin F, Laffly D, Le Ni Y (2014) A dynamic and generic cloud computing model for glaciological image processing. Int J Appl Earth Obs Geoinf 27:109–115
10. Porikli F (2005) Integral histogram: a fast way to extract histograms in cartesian spaces. In: Computer vision and pattern recognition, 2005. CVPR 2005. In: IEEE computer society conference on, vol 1. IEEE, pp 829–836
11. Rieke M, Foerster T, Geipel J, Prinz T (2011) High-precision positioning and realtime data processing of UAV systems. Int Arch Photogramm, Remote Sens Spat Inf Sci 38:1–C22
12. Shahbazi M, Théau J, Ménard P (2014) Recent applications of unmanned aerial imagery in natural resource management. GiSci Remote Sens 51(4):339–365
13. Dey N, Bhatt C, Ashour AS (2019) Big data for remote sensing: visualization, analysis and interpretation digital earth and smart earth. Springer International Publishing AG, part of Springer Nature 2019, Springer, Cham

14. Yang W, Di L (2004) An accurate and automated approach to georectication of hdf-eos swath data. Photogr Eng Remote Sens 70(4):397–404
15. Wang S, Li W, Wang F (2017) Web-scale multidimensional visualization of big spatial data to support earth sciences—a case study with visualizing climate simulation data. Informatics 4(3). https://doi.org/10.3390/informatics4030017
16. Cao X, Wu C, Lan J, Yan P, Li X (2011) Vehicle detection and motion analysis in low-altitude airborne video under urban environment. IEEE Trans Circuits Syst Video Technol 21(10):1522–1533